

ORFV: A Novel Oncolytic and Immune Stimulating Parapoxvirus Therapeutic

Julia L Rintoul¹, Chantal G Lemay¹, Lee-Hwa Tai¹, Marianne M Stanford¹, Theresa J Falls¹, Christiano T de Souza¹, Byram W Bridle², Manijeh Daneshmand¹, Pamela S Ohashi^{3,4}, Yonghong Wan², Brian D Lichty², Andrew A Mercer⁵, Rebecca C Auer¹, Harold L Atkins¹ and John C Bell¹

¹Department of Biochemistry, Microbiology & Immunology, Faculty of Medicine, University of Ottawa, Ottawa Hospital Research Institute, Centre for Innovative Cancer Research, Ottawa, Ontario, Canada; ²Department of Pathology and Molecular Medicine, Centre for Gene Therapeutics, McMaster University, Faculty of Health Sciences, Hamilton, Ontario, Canada; ³The Campbell Family Institute for Breast Cancer Research, Ontario Cancer Institute/Princess Margaret Hospital, University Health Network, Toronto, Ontario, Canada; ⁴Department of Immunology, University of Toronto, Toronto, Ontario, Canada; ⁵Department of Microbiology and Immunology, University of Otago, Dunedin, New Zealand

Replicating viruses for the treatment of cancer have a number of advantages over traditional therapeutic modalities. They are highly targeted, self-amplifying, and have the added potential to act as both gene-therapy delivery vehicles and oncolytic agents. *Parapoxvirus ovis* or Orf virus (ORFV) is the prototypic species of the *Parapoxvirus* genus, causing a benign disease in its natural ungulate host. ORFV possesses a number of unique properties that make it an ideal viral backbone for the development of a cancer therapeutic: it is safe in humans, has the ability to cause repeat infections even in the presence of antibody, and it induces a potent T_h-1-dominated immune response. Here, we show that live replicating ORFV induces an antitumor immune response in multiple syngeneic mouse models of cancer that is mediated largely by the potent activation of both cytokine-secreting, and tumoricidal natural killer (NK) cells. We have also highlighted the clinical potential of the virus by demonstration of human cancer cell oncolysis including efficacy in an A549 xenograft model of cancer.

Received 1 September 2011; accepted 18 December 2011; advance online publication 24 January 2012. doi:10.1038/mt.2011.301

INTRODUCTION

Biological therapeutics for cancer constitute an exciting alternative or complement to conventional chemo- and radiotherapies. Replicating oncolytic viruses (OVs) are particularly exciting as they have multiple features that can be exploited therapeutically. Although originally selected or engineered to directly infect and destroy cancer cells, there is accumulating evidence that OVs are acting via a number of additional mechanisms including tumor vascular disruption^{1,2} and activation of innate^{3,4} and/or adaptive antitumor immune responses.^{5,6} An example of an OV with potent antitumor immune-stimulating activity is the herpes virus-based OncoVex product that is engineered to express granulocyte-macrophage colony-stimulating factor and has recently completed

enrollment in a pivotal phase 2 human clinical trial.⁷ The ability to stimulate an innate and adaptive antitumor immune response has been identified as an important component of the therapeutic activity of several different OVs, where some of the OVs have now demonstrated efficacy even in the absence of oncolytic activity.^{3,4,8} These data, combined with the early clinical success of OVs,^{5,7,9} have highlighted the potential impact of replicating viruses for the treatment of cancer.

Parapoxvirus ovis or Orf virus (ORFV) is the prototypic member of the *Parapoxvirus* genus, and has a worldwide distribution causing acute dermal infections in its natural hosts: goat and sheep.¹⁰ The lesions caused by ORFV infection are initiated and maintained in wounded skin, and are marked by an extensive vascular proliferation and dilation which is caused partly by the expression of vascular endothelial growth factor by the viruses.¹¹ Although naive to the cancer therapeutic field, the ORFV replicative “niche” is an isolated regenerative wound with an extensive vasculature, much like a tumor microenvironment. In addition, ORFV possesses a number of unique characteristics that have not only led to the development of Parapoxviruses for antiviral vaccine platforms,^{12–14} but also suggest that it may be an excellent platform for the development of new cancer biotherapies. In contrast to zoonotic orthopoxviruses,¹⁵ human ORFV infections do not lead to serious disease.^{16–18} Additionally, ORFV treatment leads to a potent induction of a T_h-1-dominated immune response involving the accumulation of CD4⁺ and CD8⁺ T cells, B cells, natural killer (NK) cells, neutrophils, and dendritic cells (DCs),^{19–21} and cytokines including interleukin-1 β (IL-1 β), IL-8, granulocyte-macrophage colony-stimulating factor, IL-2 and interferon- γ (IFN- γ).^{10,22–25} Interestingly, these robust immune responses are associated with the viral particle itself, as numerous data have shown immune stimulation by inactivated ORFV in a number of different species,^{12,14,22,26} including humans.^{22,27,28} Importantly, the immune stimulation has been compared with other poxviruses, and in all cases the immune stimulatory profile is unique to ORFV.^{22,29,30} In addition, in contrast to cytokine therapies, ORFV T_h-1 immune-stimulation is regulated by subsequent upregulation of T_h-2 cytokines like IL-4 and IL-10.^{28,29} Lastly, an

Correspondence: John C Bell, Centre for Innovative Cancer Research, Ottawa Hospital Research Institute, 503 Smyth Road, 3rd floor ORCC, Ottawa, Ontario K1H 1C4, Canada. E-mail: jbell@ohri.ca

ORFV platform may be superior as Parapoxvirus researchers have described reoccurring infections in animals as a result of a very short-lived duration of the ORFV-specific immunity.^{15,17} Although antibody production after ORFV infection is normal, antibody appears to play little to no role in protection upon reinfection, and neutralizing antibody is rare.^{17,31,32}

We hypothesized that ORFV could be an ideal cancer therapeutic candidate considering its unique immune stimulation profile and its limited pathogenicity in humans. Here, we present data that show that ORFV induces anticancer effects in multiple syngeneic murine models of cancer, where the mechanism of action is largely attributed to potent induction of cytotoxic and cytokine-secreting NK cells. Importantly, although ORFV replicates very poorly in normal human tissues, we show that it has robust replication in a spectrum of human cancer cell lines and is therapeutically active in a human lung cancer xenograft model.

RESULTS

ORFV can reduce tumor burden in multiple mouse models of cancer

Because ORFV has been documented as an efficacious immunotherapy in a number of antiviral models,^{12–14} we wanted to first explore the *in vivo* anticancer potential of ORFV in immune-competent mouse models.^{33–36} Mice (C57Bl/6 and Balb/c) were challenged with LacZ-expressing cancer cells intravenously (i.v.)

on day 0 (**Figure 1a**). Tumor-bearing animals were then treated three times i.v. with phosphate-buffered saline (PBS) as a control, or ORFV at a dose of 10^7 plaque-forming units (p.f.u.). At 10 or 14 days after challenge, lungs were harvested and processed using a β -galactosidase-containing stain solution to visualize lung metastases. Representative images of lungs isolated from the C57Bl/6 mice at day 14 after i.v. B16F10-LacZ tumor challenge illustrate the reduction in lung tumor burden resulting from systemic delivery of ORFV (**Figure 1b**). Lung tumor burden from animals treated with PBS was quantified and compared with mice treated with one (on day 1, 3, or 8) or three doses of ORFV (**Figure 1c**). We found that even one dose of ORFV as late as 8 days after B16F10-LacZ challenge can significantly reduce the tumor burden.

A Balb/c lung model was also tested, and we found that ORFV treatment of CT26-LacZ lung tumor-bearing animals led to nearly 100% reduction in the tumor burden (**Figure 1d**). Quantification of the number of surface lung metastases demonstrated a significant reduction in tumor burden after either one or three doses of ORFV (**Figure 1e**). ORFV treatment of Balb/c mice bearing CT26-LacZ lung tumors led to a significant survival advantage (**Supplementary Figure S1a**), and intravenous ORFV therapy of subcutaneous CT26 tumors led to a significant reduction in tumor burden over time (**Supplementary Figure S1b**). Therefore, systemic ORFV treatment can significantly reduce tumor burden in multiple syngeneic immune-competent models of cancer.

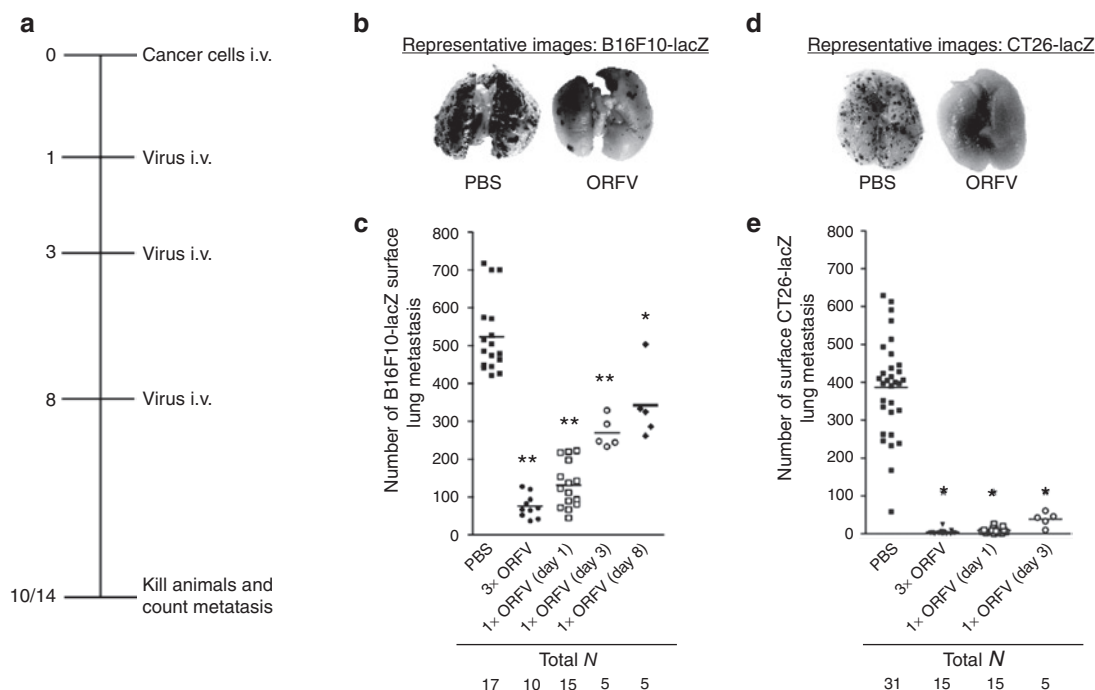


Figure 1 ORFV treatment of syngeneic murine lung models. **(a)** Schematic outlining the treatment schedule for the metastatic lung tumor models. **(b)** C57Bl/6 mice were challenged with 3×10^5 B16F10-LacZ cells i.v., and dosed one or three times with ORFV (10^7) as indicated. At day 14 after cell injection, lungs were excised and surface metastases were counted. Representative images of the lungs from animals treated with three doses of ORFV or PBS control are shown. **(c)** The number of surface lung metastases in animals treated as in **(b)**; bars represent the mean for each group ($*P < 0.01$, $**P < 0.005$ using an unpaired *t*-test with Welch's correction). **(d)** Balb/c mice were challenged with 10^5 CT26-LacZ cells i.v., and dosed one or three times with ORFV (10^7) as indicated. At day 10 after cell injection, mice were killed, their lungs processed as described above. Representative images of the lungs from animals treated with three doses of ORFV or PBS are shown. **(e)** The number of surface lung metastases in animals treated as in **(d)**; bars represent the mean for each group ($*P < 0.005$ using an unpaired *t*-test with Welch's correction). 3x ORFV refers to three doses of virus (10^7) at days 1, 3, and 8 after cell injection; 1x ORFV refers to one dose of virus (10^7) given on the indicated day. i.v., intravenous; ORFV, Orf virus; PBS, phosphate-buffered saline.

ORFV replication is required for full treatment efficacy

The mechanism of ORFV-mediated reduction in tumor burden was analyzed in both models by examining virus amplification

in vitro in the respective cancer cell lines. Phase-contrast images of B16F10-LacZ cells and CT26-LacZ cells at 48 hours postinfection showed cell rounding, indicative of a virus-induced cytopathic effect (Figure 2a). The dose dependency of ORFV-induced

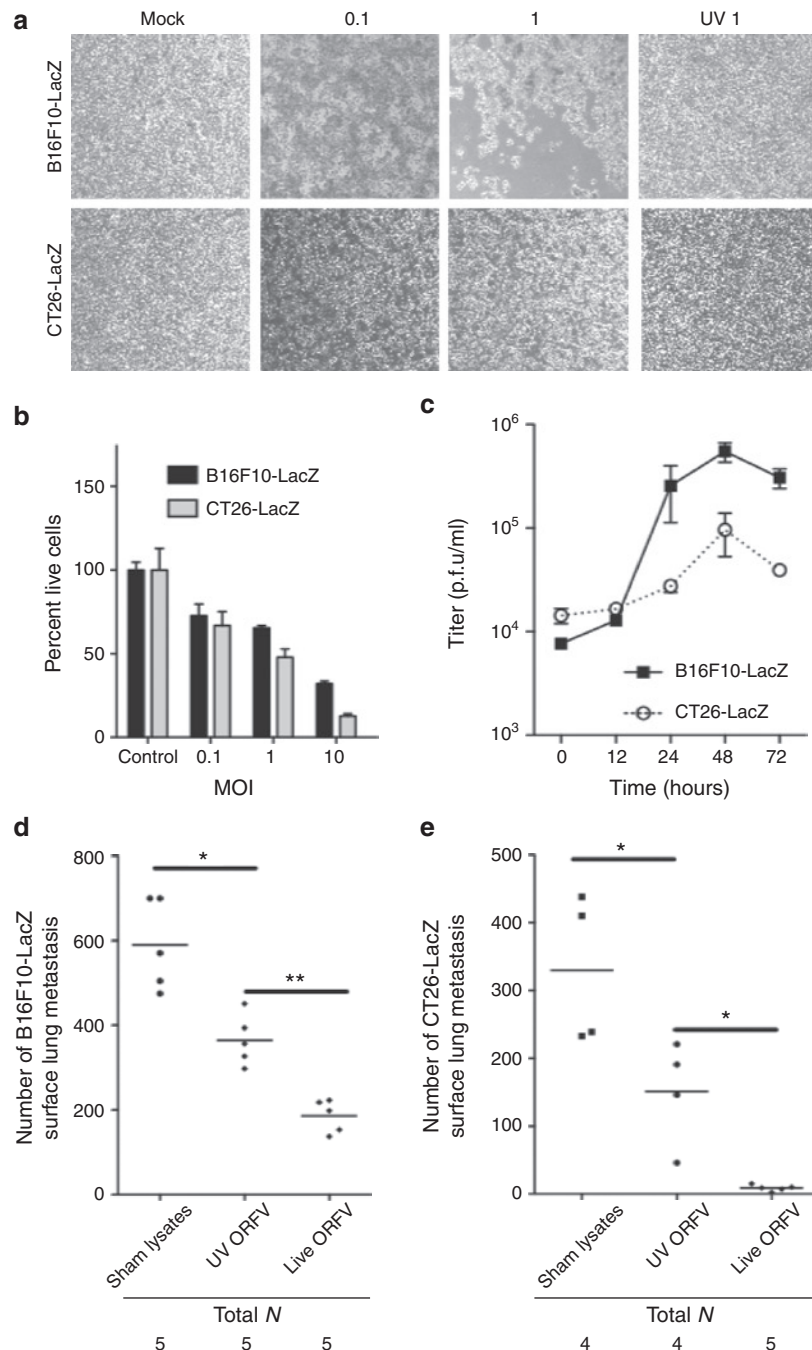


Figure 2 ORFV infection of murine cancer cells. **(a)** Phase-contrast images of mock-infected, ORFV-infected (MOI of 0.1 and 1), or UV-inactivated ORFV-infected (MOI 1) B16F10-LacZ and CT26-LacZ cells at 48 hours postinfection at a magnification of ×40. **(b)** Cytotoxicity assays of B16F10-LacZ and CT26-LacZ cells mock-infected (control) or ORFV-infected at the indicated MOI. Percent live cells was determined at 72 hours postinfection by normalization to mock-infected controls, $N = 4$, mean ± SEM. **(c)** ORFV growth curves were performed on B16F10-LacZ and CT26-LacZ cell lines at an MOI of 0.3. Cells were infected at time 0, and cell lysates collected and processed by plaque assay at time-points postinfection, $N = 2$, mean ± SEM. **(d)** C57Bl/6 mice challenged with 3×10^5 B16F10-LacZ cells intravenously (i.v.), and dosed three times with sham-infected cell lysates, live or UV-inactivated ORFV (10^7). At day 14 after cell challenge, lungs were isolated and metastases counted. Bars represent the mean for each group (* $P < 0.01$, ** $P < 0.005$ using an unpaired t -test with Welch's correction). **(e)** Balb/c mice challenged with 10^5 CT26-LacZ cells i.v., and dosed three times with sham-infected cell lysate, live or UV-inactivated ORFV (10^7). At day 10 after cell challenge, lungs were isolated and metastases counted. Bars represent the mean for each group (* $P < 0.05$ using an unpaired t -test with Welch's correction). MOI, multiplicity of infection; PBS, phosphate-buffered saline; p.f.u., plaque-forming unit; UV, ultraviolet.

cell death was quantified (Figure 2b) and found to be dependent on productive infection as ultraviolet (UV)-inactivated ORFV did not induce cytopathic effect in either cell line (Figure 2a). The amount of infectious ORFV produced by B16F10-LacZ and CT26-LacZ cancer cells was determined by multistep growth curve analysis (Figure 2c) and revealed that both cell lines can support a modest amount of virus replication. To determine whether ORFV replication was important for the *in vivo* efficacy achieved in the C57Bl/6 and Balb/c lung models, UV-inactivated ORFV was compared with live ORFV (Figure 2d,e). Quantification of the number of surface lung metastases in both models indicated that although UV-inactivated virus could significantly reduce lung metastases in these models, replicating ORFV was required to achieve maximum efficacy. Interestingly, despite only modest ORFV replication in murine cancer cell lines, ORFV therapy was as good or better than oncolytic vaccinia, Raccoonpox, and Myxoma virus (MYXV) at reducing lung metastasis in both lung models (Supplementary Figure S2), even at a log lower dose (Supplementary Figure S2b). From these data, and the observation that UV-inactivated virus has some therapeutic activity, we hypothesized that the activation of innate or adaptive immune responses by ORFV could be contributing to its anticancer activity.

***In vivo* ORFV infection of lung tumor-bearing animals correlates with clearance of lung metastases**

A tissue distribution experiment was performed to determine the kinetics of *in vivo* ORFV infection in relation to the kinetics of lung tumor clearance. Tumor-bearing C57Bl/6 mice were treated with ORFV *i.v.* at a dose of 10^7 p.f.u. on day 0, and tissues were harvested at three time-points postinfection. ORFV was recovered from the lungs at early time-points, and nearly all virus were cleared by day 5 postinfection (Figure 3a). No virus was recovered from any of the other tissues examined including spleen, liver, kidney, ovary, and brain (data not shown). Lung tumor clearance from ORFV-treated animals was found to occur primarily within the first 48 hours postinfection, evidenced by both the enumeration of lung metastasis (Figure 3b), and representative photographs of the large lobe of lungs from ORFV-treated animals (Figure 3c). The tissue distribution experiment was also performed in Balb/c mice to confirm the correlation between *in vivo* ORFV infection and tumor clearance (Supplementary Figure S3). Titer data demonstrate that virus was only recovered from the lungs of animals at day 2 postinfection, and was cleared by day 5 (Supplementary Figure S3a), and the clearance of lung metastases occurred primarily within the first 48 hours (Supplementary Figure S3b,c). A comparison of the lungs from tumor-bearing, ORFV-treated and untreated Balb/c animals demonstrated no pathological effects from the virus (Supplementary Figure S4). We used a LacZ-expressing version of ORFV to determine whether virus replication was restricted to the tumor bed. In these experiments, a B16F10 cell line lacking the LacZ transgene was used to initiate tumor formation in mouse lungs and subsequently tumor-bearing and tumor-free animals were treated with ORFV-LacZ. Significant viral infection and spread was only seen in tumor-bearing animals (Figure 3d).

***i.v.* delivery of ORFV leads to expansion and activation of innate immune cells in the spleen**

To establish the contribution of the immune system in the ORFV-mediated efficacy in the lung models, flow cytometry analysis was performed. Spleens isolated from tumor-bearing Balb/c animals showed dramatic splenomegaly at 5 days postinfection with ORFV (Figure 4a). The splenomegaly was attributed to the expansion in the number of lymphocytes in the spleen (Figure 4b). Flow cytometry analysis demonstrated a trend toward a disproportionate expansion in innate immune cells (DC and NK cells) when compared with adaptive immune cells (CD8⁺ T cells) in the spleen (Figure 4c). Expression of the early activation marker CD69 on NK cells from Balb/c splenocytes of tumor-bearing animals showed nearly 90% activation at 24 hours postinfection compared with PBS-treated animals (Figure 4d). Splenocytes from tumor-bearing C57Bl/6 animals were analyzed at several time-points postinfection where ORFV induced significantly more CD69 expression on NK cells when compared with PBS-treated animals (Figure 4e).

To determine whether the adaptive immune system was required for the ORFV efficacy, CD4⁺ or CD8⁺ T cells were depleted from ORFV-treated animals in a Balb/c CT26-LacZ survival experiment, where ORFV treatment led to a significant extension in overall survival (Supplementary Figure S5). We found that neither CD4⁺ nor CD8⁺ T cells are required for the ORFV-mediated efficacy in this model. Collectively, these data indicate that ORFV is capable of stimulating an innate immune response, which may be involved in the efficacy achieved in the C57Bl/6 and Balb/c mouse models.

Cell depletion and *ex vivo* cytotoxicity studies implicate NK cells in the efficacy achieved by ORFV

We examined the contribution of NK cells to ORFV therapy using antibody depletion studies. The dose and schedule of the NK cell-depleting antibody was tested in both C57Bl/6 and Balb/c mice (Supplementary Figure S6a,b) to ensure that the depletion was sufficient, and would last for the duration of the experiment. In both the C57Bl/6 and Balb/c lung models, NK cell depletion reduced the ability of ORFV to clear lung metastases (Figure 5a,b).

NK cell cytotoxicity assays were performed at time-points postinfection from tumor-naïve C57Bl/6 mice treated with live or UV-inactivated ORFV *i.v.* (Figure 5c,d). At 24 hours postinfection, NK cells isolated from both live and UV-inactivated ORFV-treated animals induced significant cytotoxicity of B16F10-LacZ cells (Figure 5c). NK cells isolated from live ORFV-treated animals induced significantly greater B16F10-LacZ cytotoxicity than those isolated from UV-inactivated ORFV-treated animals. At 72 hours postinfection, only live ORFV treatment resulted in significant NK cell cytotoxicity of target cells (Figure 5d). Thus, systemic ORFV treatment induces a potent cytotoxic NK cell response capable of directly killing B16F10-LacZ target cells.

ORFV induces potent cytokine expression by NK cells isolated from the spleen, blood, and lung

To determine the strength and breadth of the ORFV-mediated activation of NK cells, tissues from tumor-bearing C57Bl/6 animals were analyzed by flow cytometry at 24 hours after ORFV

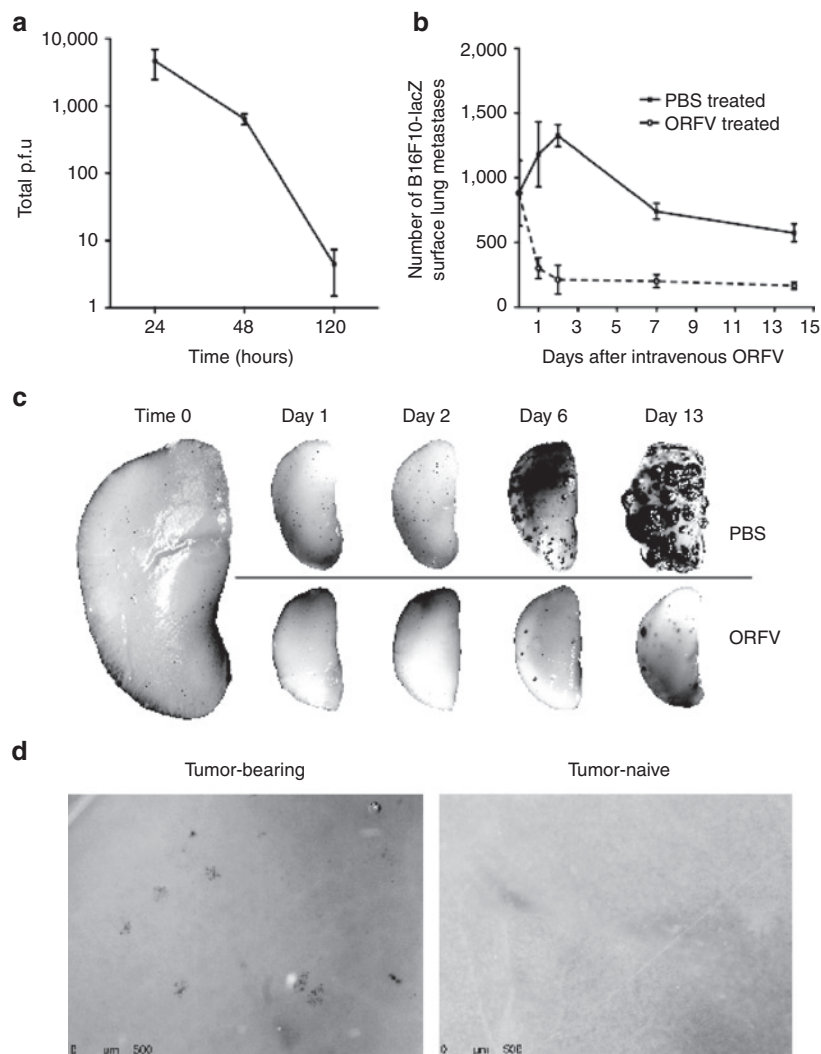


Figure 3 Kinetics of *in vivo* ORFV infection and B16F10-LacZ tumor debulking in C57Bl/6 animals. **(a)** C57Bl/6 mice were challenged with 3×10^5 B16F10-LacZ cells intravenously (i.v.) and were treated 24 hours later with ORFV-LacZ (10^7) i.v. Lung tissues were titrated for ORFV at the indicated times postinfection; $N = 3$, mean \pm SEM. **(b)** C57Bl/6 mice were challenged with 3×10^5 B16F10-LacZ cells i.v. and were treated 24 hours later with ORFV (10^7) or PBS i.v. Lung tissues were removed at various times postinfection, and the number of surface lung metastases was enumerated; $N = 3$, mean \pm SEM. **(c)** Representative images of the large lobe of lungs isolated from ORFV- or PBS-treated animals are shown at time-points postinfection. **(d)** Representative images of lungs from C57Bl/6 mice with and without B16F10 lung tumors (10^6). At day 4, animals were treated with 10^7 ORFV-LacZ i.v. Virus was detected by β -galactosidase staining at 24 hours postinfection. ORFV, Orf virus; PBS, phosphate-buffered saline; p.f.u., plaque-forming unit.

treatment for both granzyme B and IFN γ expression by NK cells (Figure 6). Importantly, these data were collected after a 5-hour GolgiPlug incubation, in the absence of any *ex vivo* stimulation. Representative histograms of lung-derived lymphocytes are illustrated in Figure 6a, demonstrating increased expression of both IFN γ and Granzyme B from NK cells isolated from ORFV-treated animals compared with PBS-treated animals. Quantification of the percent-gated NK cells secreting either granzyme B or IFN γ from the spleen, blood, and lung illustrates significant expression of both cytokines in all tissues isolated from ORFV-treated animals (Figure 6b,c, respectively). In addition, the overall amount of IFN γ and granzyme B expressed on a per cell basis was quantified (Figure 6d), where ORFV treatment also led to significant increases in the mean fluorescence intensity of both cytokines from the spleen, blood, and lung. Finally, we determined the

percent-gated NK cells that were expressing both IFN γ and granzyme B (Figure 6e). These activated NK cells were only detected in ORFV-treated animals, and were identified in all three tissues. These data underline the ability of ORFV to stimulate a potent, diverse, and systemic activation of NK cells.

Tissues from tumor-bearing C57Bl/6 animals treated with PBS or ORFV were also analyzed for CD11c expression, and corresponding expression of co-stimulatory molecules and cytokines at 24 hours after i.v. treatment (Supplementary Figure S7). There were significantly more CD11c $^+$ cells in the lung and blood of ORFV-treated animals (Supplementary Figure S7a). Dendritic cell (DC) expression of co-stimulatory molecules CD80 and CD86 were elevated in the blood and lung, and spleen, respectively (Supplementary Figure S7b,c). ORFV treatment also led to significantly more tumor necrosis factor- α and IL-12 cytokine expression from DCs in the lung

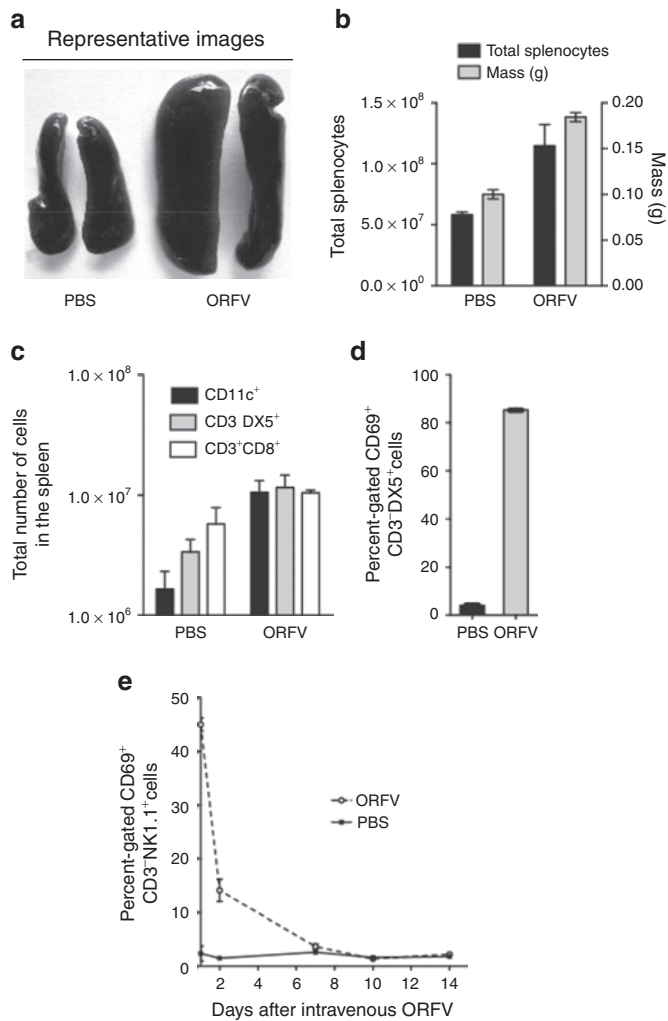


Figure 4 Expansion and activation of innate immune cells in the spleen. **(a)** Spleens isolated from tumor-bearing Balb/c animals treated with ORFV (10^7) or PBS intravenously (i.v.) were photographed at 5 days postinfection. **(b)** The mass and total number of splenocytes illustrated in **(a)** were quantified at 5 days postinfection; $N = 2$, mean \pm SEM. **(c)** The total number of dendritic cells (CD11c⁺), natural killer cells (CD3⁺DX5⁺) and cytotoxic T cells (CD3⁺CD8⁺) were quantified from spleens isolated from tumor-bearing Balb/c mice treated i.v. with ORFV (10^7) or PBS i.v. at 5 days postinfection, $N = 2$, mean \pm SEM. **(d)** CD69 expression was quantified from splenic natural killer cells (CD3⁺DX5⁺) isolated from tumor-bearing Balb/c mice 24 hours after ORFV (10^7) or PBS i.v. administration, $N = 2$, mean \pm SEM. **(e)** CD69 expression was quantified from splenic natural killer cells (CD3⁺NK1.1⁺) isolated from tumor-bearing C57Bl/6 mice at time-points after i.v. ORFV (10^7) or PBS treatment, $N = 3$, mean \pm SEM. ORFV, Orf virus; PBS, phosphate-buffered saline.

(Supplementary Figure S7d,e). To rule out virus amplification in murine immune cells, ORFV infection of both DCs and NK cells was also analyzed. At 24 hours postinfection, there was no ORFV amplification in either cell type (Supplementary Figure S7f).

ORFV therapy reduces tumor burden in an A549 xenograft model of cancer

To evaluate the clinical potential of the virus, *in vitro* growth curve analysis was performed on a panel of human cancer cells lines, and the fold-increase in virus production was determined (Figure 7a).

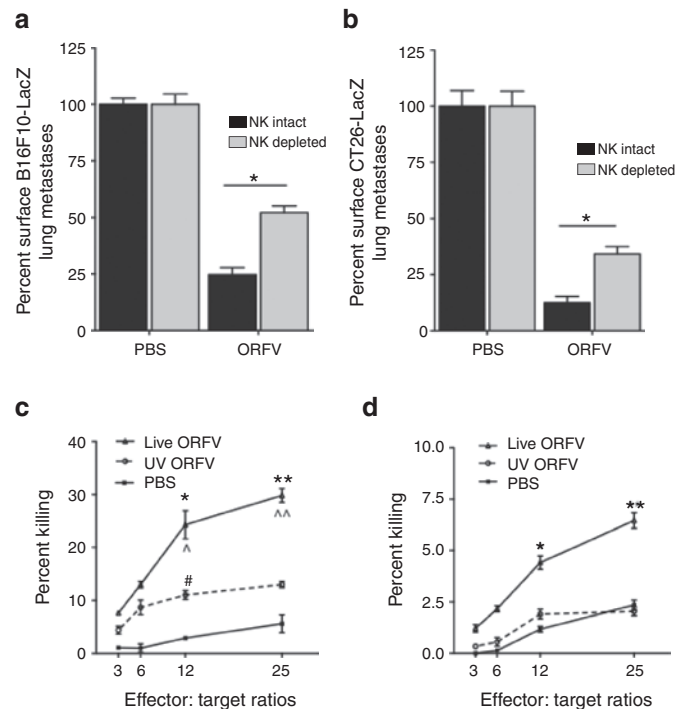


Figure 5 ORFV activation of NK cells is contributing to efficacy achieved in the lung models. **(a)** C57Bl/6 animals treated intravenously (i.v.) with three doses of PBS or ORFV (10^7) were depleted of NK cells using an optimized dose and schedule of anti-asialo i.v. or control IgG antibody. Animals were killed at 14 days after cell injection, lungs were isolated and processed, and the number of surface lung metastases was quantified, $N = 5$, mean \pm SEM ($*P < 0.0005$ using an unpaired *t*-test with Welch's correction). **(b)** Balb/c animals treated i.v. with three doses of PBS or ORFV (10^7) were depleted of NK cells using an optimized dose and schedule of anti-asialo i.v. or control IgG antibody. Animals were killed at 10 days after cell injection, lungs were isolated and processed, and the number of surface lung metastases was quantified, $N = 10$, mean \pm SEM ($*P < 0.05$ using an unpaired *t*-test with Welch's correction). *Ex vivo* cytotoxicity assays were performed on NK cells isolated from ORFV- or PBS-treated C57Bl/6 mice. Spleens were isolated, pooled, and enriched for NK cells by DX5⁺ cell sorting. NK cells were then mixed with chromium-labeled B16F10-LacZ target cells in triplicate, at different effector:target ratios. **(c)** Shown is the percent killing of target B16F10-LacZ cells at 24 hours postinfection, $N = 3$, mean \pm SEM ($*P < 0.05$, $**P < 0.005$ comparing live ORFV with PBS, $^{\wedge}P < 0.05$, $^{\wedge\wedge}P < 0.01$ comparing live ORFV with UV ORFV, $*P < 0.05$ comparing UV ORFV with PBS, using an unpaired *t*-test with Welch's correction). **(d)** Shown is the percent killing of target B16F10-LacZ cells at 72 hours postinfection, $N = 3$, mean \pm SEM ($*P < 0.05$, $**P < 0.05$ using an unpaired *t*-test with Welch's correction). NK, natural killer; ORFV, Orf virus; PBS, phosphate-buffered saline; UV, ultraviolet.

ORFV was able to productively infect 9 of the 13 cell lines tested with over three-log output in A549 lung adenocarcinoma cells. ORFV growth curve analysis of infected A549 cancer cells and normal human dermal fibroblast cells highlights the preferential cytotoxicity and amplification in cancer cells (Figure 7b,c). To test ORFV *in vivo*, CD-1 nude mice were engrafted with A549 cells subcutaneously, and mice were treated intratumorally with five doses of ORFV (10^7) or PBS vehicle control. ORFV was able to significantly reduce A549 tumor burden as illustrated by tumor volume measurements (Figure 7d). Collectively, these data highlight the potential of ORFV as a replicating therapeutic for the treatment of human cancer.

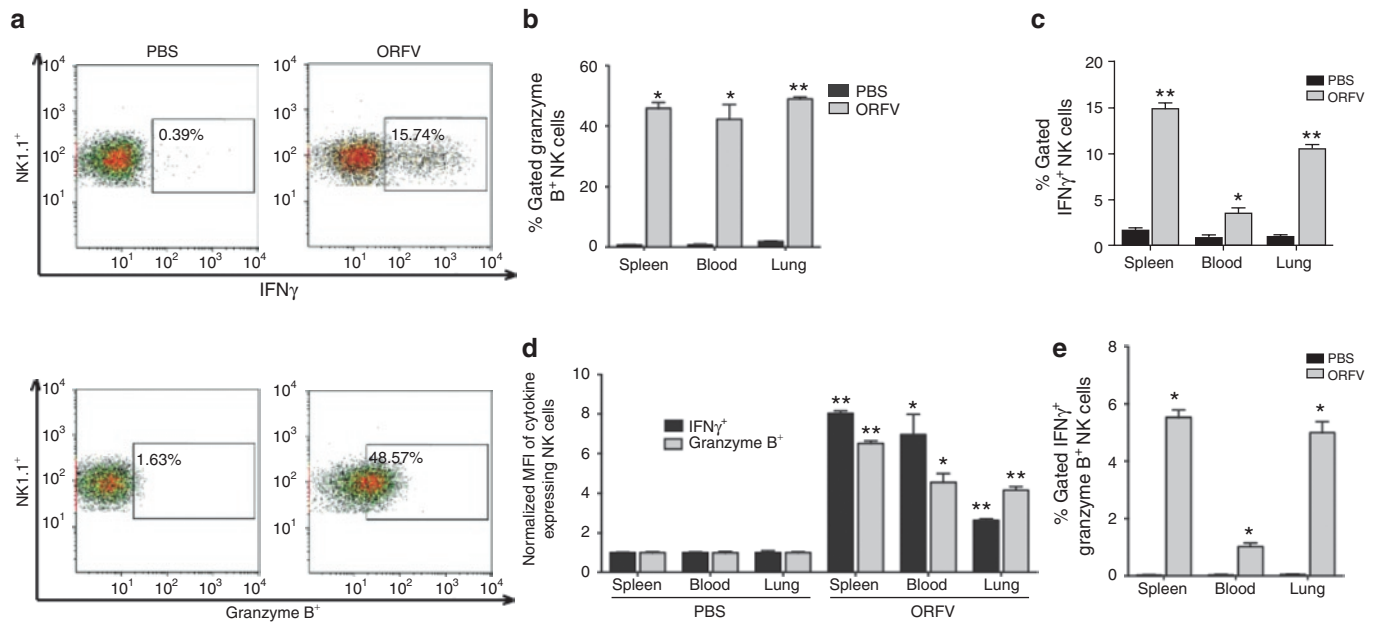


Figure 6 Flow cytometry analysis of ORFV-activated NK cells. **(a)** Tumor-bearing C57Bl/6 animals were treated intravenously (i.v.) with 10^7 ORFV or PBS. At 24 hours postinfection, tissues were harvested from animals, and processed by flow cytometry. Representative histograms of lymphocytes isolated from the lung of animals treated with PBS or ORFV are shown. **(b)** Percent-gated granzyme B expression from NK cells isolated from the spleen, blood, and lung of ORFV- and PBS-treated animals is compared, $N = 4$, mean \pm SEM ($*P < 0.005$, $**P < 0.0001$ using an unpaired t -test with Welch's correction). **(c)** Percent-gated IFN γ expression from NK cells isolated from the spleen, blood, and lung of ORFV- and PBS-treated animals is compared, $N = 4$, mean \pm SEM ($*P < 0.05$, $**P < 0.0005$ using an unpaired t -test with Welch's correction). **(d)** The amount of granzyme B and IFN γ expressed on per NK cell basis was determined using the mean fluorescence intensity (MFI). Data are shown as the fold-increase in MFI compared with PBS-treated animals, $N = 4$, mean \pm SEM ($*P < 0.01$, $**P < 0.0005$ using an unpaired t -test with Welch's correction). **(e)** Percent-gated NK cells expressing both granzyme B and IFN γ were compared for lymphocytes isolated from PBS- and ORFV-treated animals, $N = 4$, mean \pm SEM ($*P < 0.005$). IFN γ , interferon- γ ; NK, natural killer; ORFV, Orf virus; PBS, phosphate-buffered saline.

DISCUSSION

We have identified and characterized the anticancer properties of a new poxvirus platform and show that ORFV treatment of both immune-competent and xenograft human tumor models leads to significant antitumor activity. Our results implicate NK cells in the ORFV-mediated reduction in tumor burden (Figure 4–6). In addition, we demonstrated by both expression of co-stimulatory molecules, and cytokines (Supplementary Figure S7) that ORFV therapy induces the activation of DCs. The exact mechanism by which ORFV stimulates the immune system is not yet known, but both TLR-dependent and independent mechanisms have been described including signaling via CD14.^{28,29} It is possible, therefore, that NK cell activation by ORFV is indirect via DC activation, as previous reports have highlighted DC–NK cross-talk mechanisms induced by other OVs.³⁷

In earlier studies, inactivated ORFV particles on their own were shown to stimulate a T_H -1-dominated immune response,^{12,14,22} and so it was not surprising that UV-inactivated ORFV had a significant impact in the metastatic lung models (Figure 2d,e). Replicating ORFV, however, has a significantly greater impact in the lung models; possibly due to its induction of a more potent cytotoxic NK cell response (Figure 5c,d), coupled with its oncolytic activity in the murine cancer cells (Figure 2c). A number of OVs have been shown to induce potent adaptive antitumor immune responses (reviewed by Melcher *et al.*³⁸), but only a select few have been shown to stimulate NK cell responses.^{3,4,37} Because cytokine production by NK cells supports T_H -1 immunity,³⁹ the induction of IFN γ -secreting

NK cells suggests that ORFV treatment could also lead to adaptive antitumor immune responses. Interestingly, several reports have now indicated that human⁴⁰ and mouse⁴¹ NK cells can be divided into two phenotypically distinct subsets: poorly cytotoxic, cytokine-producing NK cells, and highly cytotoxic, poor cytokine-producing NK cells. Remarkably, we have shown that ORFV is capable of stimulating NK cells of both phenotypes (Figure 5,6).

In our preclinical studies, we observed significant increases in the size of spleens in ORFV-treated mice and this could represent a potential site for an adverse reaction. However, the splenomegaly was transient as immune cell populations returned to their normal proportions within 8 days after treatment. Kinetic studies have found that the ORFV-induced proinflammatory stimulation is balanced with subsequent induction of an anti-inflammatory response.^{28,29} We believe that the unique biology of ORFV that allows for self-regulation of inflammatory responses can be exploited for safe and effective therapeutic benefit as we describe herein.

From a clinical perspective, we are encouraged that ORFV efficacy in murine lung tumor models was comparable or better than three other oncolytic poxviruses (Supplementary Figure S2), and that ORFV was able to infect a panel of human cancer cell lines (Figure 7a). In the literature, it has only ever been documented that ORFV can productively infect primary cell cultures prepared from bovine testis.^{11,42,43} Our findings that a number of human tumor cell lines are permissive for ORFV replication is reminiscent of the earlier studies with MYXV that had documented a restricted host range of the virus, and later found MYXV to

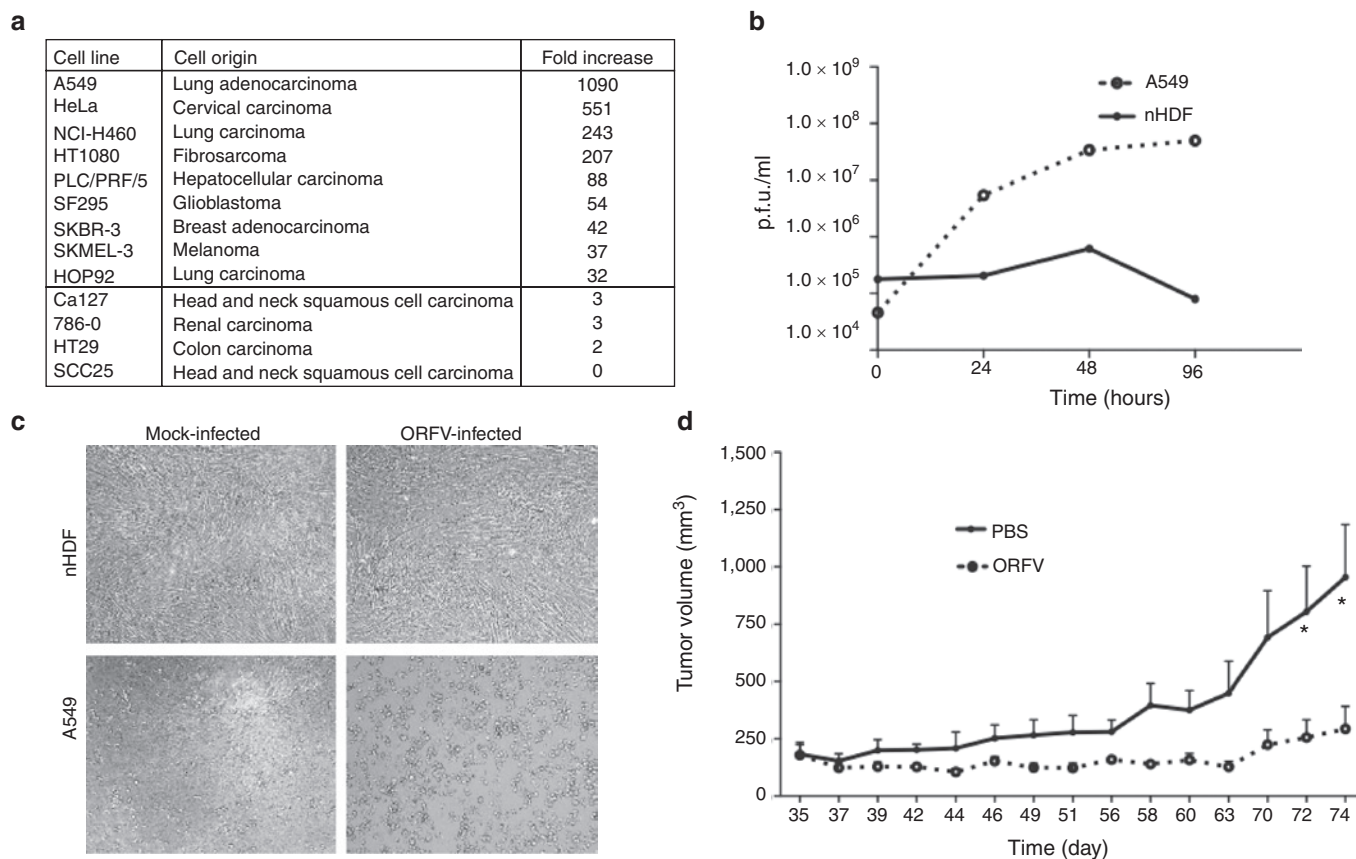


Figure 7 ORFV treatment of human xenograft tumors. **(a)** ORFV growth curves were performed on a panel of human cancer cell lines at an MOI of 1. Cells were infected at time 0, and cell lysates collected and processed for virus by OA3.Ts plaque assay at time-points postinfection. Virus titer was compared with input titers at 72 hours postinfection to calculate the fold-increase in ORFV. **(b)** Representative ORFV growth curves on A549 and nHDF cells at an MOI of 1. **(c)** Phase-contrast images of mock-infected and ORFV-infected A549 and nHDF cells at an MOI of 0.05, at 72 hours postinfection at a magnification of $\times 40$. **(d)** Human A549 cells (2×10^6) were seeded subcutaneously into the right flank of CD-1 nude mice. ORFV (10^7) or PBS treatments were given intratumorally on days 24, 27, 29, 31, and 34 after tumor implantation. Mouse tumor volume was monitored over time, $N = 5$, mean \pm SEM ($*P < 0.05$ using an unpaired t -test with Welch's correction). MOI, multiplicity of infection; nHDF, normal human dermal fibroblast; ORFV, Orf virus; PBS, phosphate-buffered saline; p.f.u., plaque-forming unit.

replicate well in human cancer cells.⁴⁴ Our data suggest, therefore, that like other OV, ORFV may naturally be selective for cancer cell replication supported by alterations in signal-transduction pathways, like activated AKT for MYXV,⁴⁴ and defects in IFN signaling for vesicular stomatitis virus.⁴⁵ Indeed, we show here that ORFV can replicate in A549 cells and when engrafted into nude mice, has readily apparent antitumor activity *in vivo* (Figure 7d). These data emphasize ORFV's potential as a multimodality viral therapy for humans, where the virus could have both an oncolytic impact and potentially induce even greater immune responses than those reported here in the murine models.

The potential of ORFV in the activation of NK cells and human cancer cell oncolysis highlight the novel anticancer potential of the virus. Because antibody has been reported to be a barrier to OV therapy,⁴⁶ it is advantageous that the majority of the population has had limited exposure to ORFV, and that antibody does not prevent reoccurring infections in animals.^{15,17,31,32} These characteristics, combined with the unique biology of the ORFV virion and its limited pathogenicity in humans, make it an attractive platform for the development of new anticancer biotherapeutics.

MATERIALS AND METHODS

Cell lines. Human and murine cell lines were maintained in Dulbecco's modified Eagle's medium (HyClone, Logan, UT) supplemented with 10% fetal calf serum (PAA Laboratories, Etobicoke, Ontario, Canada), and grown at 37°C and 5% CO₂. B16F10-LacZ cells were generated by stable transfection with LacZ complementary DNA, as described earlier.⁴⁷ Human tumor cell lines were from the NCI-60 reference panel: A549, HeLa, NCI-H460, HT1080, PLC/PRF/5, SF295, SKBR-3, SKMEL-3, HOP92, Cal27, 786-0, HT29, and SCC25. CT26.CL25 (CT26-LacZ), CT26, B16F10, and OA3.Ts were purchased from ATCC (Manassas, VA). Normal human dermal fibroblast cell cells were purchased from Cascade Biologics (Burlington, Ontario, Canada).

Viruses. Wild-type ORFV strain NZ2 and ORFV-LacZ (vascular endothelial growth factor-deleted LacZ-expressing ORFV) strain NZ2^{11,42} were obtained from Dr Andrew Mercer (University of Otago, Dunedin, New Zealand). Oncolytic vaccinia virus, Raccoonpox and MYXV have been described previously.³⁴

ORFV production, UV inactivation, and titering. Viral stocks were prepared by the infection of confluent OA3.Ts at a multiplicity of infection of 0.05. Cells and supernatants were harvested following a 5-day infection at 37°C, 5% CO₂ by gentle cell scraping. Cell lysates were collected by centrifugation, and resuspended in 1 mmol/l TRIS pH 9.0, and subjected to three

freeze-thaw cycles. Cell debris was removed by centrifugation, and lysates dounce homogenized before sucrose cushion purification in a JS-13.1 rotor at 11,500 r.p.m. for 1.5 hours at 4°C. Virus stocks were resuspended in PBS. Sham-infected OA3.Ts were processed as described above, and were used as vehicle control treatments. Inactivation of virus was performed on ORFV preparations at a concentration of 10^8 p.f.u./ml in PBS using UV-C irradiation in the Spectrolinker XL-1000 UV crosslinker (Spectronics, Westbury, NY) for 300 seconds. Confirmation of virus inactivation was measured by plaque assay before use. ORFV was titered on confluent monolayers of OA3.Ts using a carboxymethylcellulose overlay. Plaques were visualized following a 7-day incubation at 37°C by removal of overlay, and staining with 1% crystal violet (in 80% methanol). Vascular endothelial growth factor-deleted, LacZ-expressing ORFV plaques were visualized using a β -galactosidase-containing stain solution, as described previously.⁴⁸

Animals. Female 6- to 8-week-old C57Bl/6, Balb/c and CD-1 nude mice were supplied by Charles River Canada (St Constant, Quebec, Canada), and were housed in a level 2 biocontainment facility at the Animal Care and Veterinary Services within the University of Ottawa. All animal experiments were conducted in accordance with the Animal Care and Veterinary Services standard operating procedures.

In vitro viral infections. For growth curve analysis, confluent monolayers of cells were infected in a minimal volume for 1 hour at 37°C and 5% CO₂. The viral inoculum was then removed, and replaced with Dulbecco's modified Eagle's medium 10% fetal calf serum. Cells and supernatants were harvested from wells at 0, 12, 24, 48, 72, and 96 hours postinfection. Cell lysates were subjected to three freeze-thaw cycles, and titered on OA3.Ts. Cytotoxicity was assessed in 96-well plates, using alamarBlue (AbD Serotec, Raleigh, NC) after a 72-hour infection period. NK cells were isolated from the spleens of C57Bl/6 mice by negative selection using magnetic sorting and the NK Isolation Kit (Miltenyi Biotec, Auburn, CA). DCs were isolated from C57Bl/6 mice using methods described previously.³⁷

In vivo tumor models. For murine lung models, 10^5 CT26-LacZ cells were injected i.v. into Balb/c mice. Similarly, a density of 3×10^5 B16F10-LacZ cells was injected i.v. into C57Bl/6 mice. Mice were then treated i.v. with 1–3 doses of 10^7 p.f.u. ORFV in 100 μ l of PBS, or control treated (100 μ l of PBS or sham-infected lysates), on days 1, 3, and/or 8. At 10 days after CT26-LacZ injection, and 14 days after B16F10-LacZ injection, mice were anesthetized with Euthanyl, and lungs were harvested and stained with a β -galactosidase solution.³³ The number of lung metastases was determined by separation of lung lobes, and enumeration under a dissection microscope (Leica, Richmond Hill, Ontario, Canada). For Balb/c CT26-LacZ lung model survival experiments, animals were treated i.v. with three doses of 10^7 p.f.u. ORFV or control (100 μ l of PBS), and were monitored for signs of respiratory distress. For the Balb/c CT26 subcutaneous tumor experiment, animals were challenged with 3×10^5 CT26 cells in the right flank, and were treated i.v. with 5 doses of 10^7 p.f.u. ORFV in 100 μ l of PBS, or control treated (100 μ l of PBS) on days 10, 14, 17, 21, and 24 after tumor implantation. For CD-1 nude xenograft experiments, 2×10^6 A549 cells were injected subcutaneously into the right flank of mice. At 23 days postimplantation, mice were treated intratumorally with five doses of 10^7 ORFV or PBS control. Subcutaneous tumors were measured 2–3 times per week using digital calipers. Animals were killed when tumor burden reached a volume of 1,500 mm³.

Tissue distribution experiments. To determine the kinetics of the *in vivo* ORFV infection, lung tumor-bearing C57Bl/6 and Balb/c mice were treated with 10^7 p.f.u. of ORFV-LacZ i.v. Organs were then harvested from animals at specified time-points after infection. Tissues were first homogenized, and subjected to three freeze-thaw cycles before OA3.Ts plaque assay, as described above. To allow visualization of plaques at the lowest dilution in the presence of tissue debris, plaques were visualized using an β -galactosidase-containing staining solution.⁴⁸ To examine the pathology of lung tissues after ORFV therapy, Balb/c mice ($N = 2$) were challenged i.v.

with 10^5 CT26-LacZ cells, followed by i.v. PBS or 10^7 ORFV at 24 hours. At 72 hours, animals were killed, and lungs isolated, fixed, and embedded in paraffin. Hematoxylin-and-eosin-stained sections of lung tissues were examined by a pathologist in a blinded fashion. Images were captured using Aperio ScanScope (Aperio Technologies, Vista, CA) and analyzed using a Aperio ImageScope software.

Flow cytometry. To analyze splenic lymphocyte populations (Figure 4) spleens were removed from animals, photographed, weighed, and red blood cells lysed using ACK lysis buffer (0.15 mol/l NH₄Cl, 10 mmol/l KHCO₃, 0.1 mmol/l Na₂EDTA). Splenic lymphocytes were then analyzed for total number of NK, DC, and CD8⁺ T cells, and CD69 expression by flow cytometry using the following antibodies: CD49b-PE (Clone DX5), CD3-PE (Clone 17A2), CD8-PECy5 (Clone 53-6.7) and CD69-FITC (Clone H1.2F3) from BD Biosciences (Mississauga, Ontario, Canada) and CD11c-FITC (Clone N418; eBioscience, San Diego, CA). NK cell cytokine secretion was examined in lymphocytes isolated from the spleen, blood, and lung of tumor-bearing C57Bl/6 animals (Figure 6) following a 5-hour GolgiPlug (BD Bioscience) incubation using the following antibodies: CD3-PerCP (clone 17A2; R&D Systems, Minneapolis, MN), and NK1.1-PE (Clone PK136), Granzyme B-AF700 (Clone GB11), and IFN γ -AF647 (Clone XMG1.2) from BD Bioscience. DC cytokine expression was examined from lymphocytes isolated from the spleen, blood, and lung of tumor-bearing C57Bl/6 animals (Supplementary Figure S7) following a 5-hour GolgiPlug (BD Bioscience) incubation using the following antibodies: CD11c-PECy7 (Clone N418), CD80-PE (Clone 16-10A1), CD86-PE (Clone GL-1), TNF α -FITC (Clone MP6-XT22) from eBioscience, and IL-12-APC (Clone C15.6; BD Bioscience). Experiments were performed on a Beckman Coulter CyAn and data analyzed using Kaluza software (version 1.1; Beckman Coulter, Brea, CA).

Cell depletion tumor models. NK cell depletion experiments were performed using an optimized dose and schedule of anti-asialo GM-1 (Cedarlane, Burlington, Ontario, Canada), or Rat IgG1 κ isotype control (BD Bioscience): 25 μ l i.v. on days -4, -1, 2, 6, 9, and 13 where cancer cell injection and first ORFV treatment occur on days 0 and 1, respectively. NK cell depletion was confirmed at day 0 (before the beginning of the experiment) in both C57Bl/6 and Balb/c mice (Supplementary Figure S6). To allow for similar tumor burden in animals treated with the NK-depleting antibody, the challenge dose of B16F10-LacZ and CT26-LacZ was reduced in the NK-depleted animals to 9×10^4 and 5×10^4 , respectively. CD4⁺ and CD8⁺ T cells were depleted in Balb/c mice using reagents and dose regimes established previously.⁴⁹

NK cytotoxicity assays. Splenocytes were isolated from tumor naive ORFV- or PBS-treated C57Bl/6 mice at time-points postinfection. Isolated lymphocytes were pooled, and DX5-sorted (DX5 positive selection Kit; Miltenyi Biotec) on an Automacs Pro cell sorter (Miltenyi Biotec). B16F10-LacZ cells were harvested and labeled with Chromium-51 (Perkin Elmer, Waltham, MA) in the form of Na₂CrO₄ at 100 μ Ci for 60 minutes at 37°C. Sorted NK cells from ORFV- or PBS-treated animals resuspended at a concentration of 2.5×10^6 cells/ml and mixed with target B16F10-LacZ, which were resuspended at a concentration of 5×10^4 cells/ml at different effector-to-target ratios (50:1, 25:1, 12:1, and 6:1). The mixture was incubated for 4 hours before the analysis of chromium release in the supernatant using a gamma counter (Perkin Elmer).

SUPPLEMENTARY MATERIAL

Figure S1. ORFV efficacy in two additional Balb/c tumor models.

Figure S2. ORFV efficacy compared with other oncolytic viruses.

Figure S3. Kinetics of *in vivo* ORFV infection and CT26-LacZ tumor debulking in Balb/c animals.

Figure S4. H&E staining of lung tissues from ORFV- and control-treated Balb/c animals.

Figure S5. *In vivo* ORFV efficacy in the absence of T cells.

Figure S6. Flow cytometry analysis to test for NK cell depletion.

Figure S7. Flow cytometry analysis of ORFV activated dendritic cells.

ACKNOWLEDGMENTS

J.L.R. and C.G.L. are supported by CIHR Doctoral awards: Frederick Banting and Charles Best Canada Graduate Scholarship. L.-H.T. is supported by a Fonds de Recherche Sante Quebec—postdoctoral fellowship. This work was supported by grants from the Terry Fox Foundation (J.C.B. and H.L.A.), Ontario Institute for Cancer Research (P.S.O., H.L.A., R.C.A., J.C.B., B.D.L. and Y.W.), Canadian Cancer Society (B.D.L.), Canadian Institutes of Health Research (J.C.B. and H.L.A.), and from the Health Research Council of New Zealand (A.A.M.). Thanks to Harman Sekhon for his technical expertise and Ellena Whelan for her guidance, and technical expertise. Thanks to Kelley Parato for editing the manuscript.

REFERENCES

- Breitbach, CJ, Paterson, JM, Lemay, CG, Falls, TJ, McGuire, A, Parato, KA *et al.* (2007). Targeted inflammation during oncolytic virus therapy severely compromises tumor blood flow. *Mol Ther* **15**: 1686–1693.
- Breitbach, CJ, De Silva, NS, Falls, TJ, Aladi, U, Evgin, L, Paterson, J *et al.* (2011). Targeting tumor vasculature with an oncolytic virus. *Mol Ther* **19**: 886–894.
- Prestwich, RJ, Ilett, EJ, Errington, F, Diaz, RM, Steele, LP, Kottke, T *et al.* (2009). Immune-mediated antitumor activity of reovirus is required for therapy and is independent of direct viral oncolysis and replication. *Clin Cancer Res* **15**: 4374–4381.
- Apostolidis, L, Schirmacher, V and Fournier, P (2007). Host mediated anti-tumor effect of oncolytic Newcastle disease virus after locoregional application. *Int J Oncol* **31**: 1009–1019.
- Mastrangelo, MJ, Maguire, HC Jr, Eisenlohr, LC, Laughlin, CE, Monken, CE, McCue, PA *et al.* (1999). Intratumoral recombinant GM-CSF-encoding virus as gene therapy in patients with cutaneous melanoma. *Cancer Gene Ther* **6**: 409–422.
- Bridle, BW, Hanson, S and Lichty, BD (2010). Combining oncolytic virotherapy and tumour vaccination. *Cytokine Growth Factor Rev* **21**: 143–148.
- Kaufman, HL and Bines, SD (2010). OPTIM trial: a Phase III trial of an oncolytic herpes virus encoding GM-CSF for unresectable stage III or IV melanoma. *Future Oncol* **6**: 941–949.
- Gaivo, F, Diaz, RM, Wongthida, P, Thompson, J, Kottke, T, Barber, G *et al.* (2010). Single-cycle viral gene expression, rather than progressive replication and oncolysis, is required for VSV therapy of B16 melanoma. *Gene Ther* **17**: 158–170.
- Breitbach, CJ, Burke, J, Jonker, D, Stephenson, J, Haas, AR, Chow, LQ *et al.* (2011). Intravenous delivery of a multi-mechanistic cancer-targeted oncolytic poxvirus in humans. *Nature* **477**: 99–102.
- Haig, D, McInnes, C, Deane, D, Lear, A, Myatt, N, Reid, H *et al.* (1996). Cytokines and their inhibitors in orf virus infection. *Vet Immunol Immunopathol* **54**: 261–267.
- Savory, LJ, Stacker, SA, Fleming, SB, Niven, BE and Mercer, AA (2000). Viral vascular endothelial growth factor plays a critical role in orf virus infection. *J Virol* **74**: 10699–10706.
- Schütze, N, Raue, R, Büttner, M and Alber, G (2009). Inactivated parapoxvirus ovis activates canine blood phagocytes and T lymphocytes. *Vet Microbiol* **137**: 260–267.
- Weber, O, Siegling, A, Friebe, A, Limmer, A, Schlapp, T, Knolle, P *et al.* (2003). Inactivated parapoxvirus ovis (Orf virus) has antiviral activity against hepatitis B virus and herpes simplex virus. *J Gen Virol* **84**(Pt 7): 1843–1852.
- Fachinger, V, Schlapp, T, Strube, W, Schmeer, N and Saalmüller, A (2000). Poxvirus-induced immunostimulating effects on porcine leukocytes. *J Virol* **74**: 7943–7951.
- Czerny, CP, Zeller-Lue, C, Eis-Hübinger, AM, Kaaden, OR and Meyer, H (1997). Characterization of a cowpox-like orthopox virus which had caused a lethal infection in man. *Arch Virol Suppl* **13**: 13–24.
- Robinson, AJ and Petersen, GV (1983). Orf virus infection of workers in the meat industry. *N Z Med J* **96**: 81–85.
- Haig, DM and Mercer, AA (1998). Ovine diseases. Orf. *Vet Res* **29**: 311–326.
- Lederman, ER, Green, GM, DeGroot, HE, Dahl, P, Goldman, E, Greer, PW *et al.* (2007). Progressive ORF virus infection in a patient with lymphoma: successful treatment using imiquimod. *Clin Infect Dis* **44**: e100–e103.
- Lear, A, Hutchinson, G, Reid, H, Norval, M, and Haig, D (1996). Phenotypic characterisation of the dendritic cells accumulating in ovine dermis following primary and secondary orf virus infections. *Eur J Dermatol* **6**: 135–140.
- Jenkinson, DM, McEwen, PE, Onwuka, SK, Moss, VA, Elder, HY, Hutchinson, G *et al.* (1990). The pathological changes and polymorphonuclear and mast cell responses in the skin of specific pathogen-free lambs following primary and secondary challenge with orf virus. *Vet Dermatol* **2**: 1–9.
- Jenkinson, DM, Hutchison, G and Reid, H (1992). The B and T cell responses to orf virus infection. *Vet Derm* **3**: 57–64.
- Büttner, M, Czerny, CP, Lehner, KH and Wertz, K (1995). Interferon induction in peripheral blood mononuclear leukocytes of man and farm animals by poxvirus vector candidates and some poxvirus constructs. *Vet Immunol Immunopathol* **46**: 237–250.
- Haig, DM, Hutchinson, G, Thomson, J, Yirrell, D and Reid, HW (1996). Cytolytic activity and associated serine protease expression by skin and afferent lymph CD8+ T cells during orf virus reinfection. *J Gen Virol* **77** (Pt 5): 953–961.
- Haig, DM and McInnes, CJ (2002). Immunity and counter-immunity during infection with the parapoxvirus orf virus. *Virus Res* **88**: 3–16.
- Haig, D, Deane, D, Percival, A, Myatt, N, Thomson, J, Inglis, L *et al.* (1996). The cytokine response of afferent lymph following orf virus reinfection of sheep. *Vet Dermatol* **7**: 11–20.
- Mayr, A, Büttner, M, Wolf, G, Meyer, H and Czerny, C (1989). [Experimental detection of the paraspecific effects of purified and inactivated poxviruses]. *Zentralblatt Veterinärmedizin Reihe B* **36**: 81–99.
- Yirrell, DL, Vestey, JP and Norval, M (1994). Immune responses of patients to orf virus infection. *Br J Dermatol* **130**: 438–443.
- Friebe, A, Siegling, A, Friederichs, S, Volk, HD and Weber, O (2004). Immunomodulatory effects of inactivated parapoxvirus ovis (ORF virus) on human peripheral immune cells: induction of cytokine secretion in monocytes and Th1-like cells. *J Virol* **78**: 9400–9411.
- Friebe, A, Friederichs, S, Scholz, K, Janssen, U, Scholz, C, Schlapp, T *et al.* (2011). Characterization of immunostimulatory components of orf virus (parapoxvirus ovis). *J Gen Virol* **92**(Pt 7): 1571–1584.
- Sullivan, JT, Mercer, AA, Fleming, SB and Robinson, AJ (1994). Identification and characterization of an orf virus homologue of the vaccinia virus gene encoding the major envelope antigen p37K. *Virology* **202**: 968–973.
- Czerny, CP, Waldmann, R and Scheubeck, T (1997). Identification of three distinct antigenic sites in parapoxviruses. *Arch Virol* **142**: 807–821.
- Buddle, BM, Dellers, RW and Schurig, GG (1984). Contagious ecthyma virus-vaccination failures. *Am J Vet Res* **45**: 263–266.
- Stanford, MM, Shaban, M, Barrett, JW, Werden, SJ, Gilbert, PA, Bondy-Denomy, J *et al.* (2008). Myxoma virus oncolysis of primary and metastatic B16F10 mouse tumors in vivo. *Mol Ther* **16**: 52–59.
- Evgin, L, Vähä-Koskela, M, Rintoul, J, Falls, T, Le Boeuf, F, Barrett, JW *et al.* (2010). Potent oncolytic activity of raccoonpox virus in the absence of natural pathogenicity. *Mol Ther* **18**: 896–902.
- Wang, M, Bronte, V, Chen, PW, Gritz, L, Panicali, D, Rosenberg, SA *et al.* (1995). Active immunotherapy of cancer with a nonreplicating recombinant fowlpox virus encoding a model tumor-associated antigen. *J Immunol* **154**: 4685–4692.
- Epaulard, O, Toussaint, B, Quenee, L, Derouazi, M, Bosco, N, Villiers, C *et al.* (2006). Anti-tumor immunotherapy via antigen delivery from a live attenuated genetically engineered *Pseudomonas aeruginosa* type III secretion system-based vector. *Mol Ther* **14**: 656–661.
- Boudreau, JE, Stephenson, KB, Wang, F, Ashkar, AA, Mossman, KL, Lenz, LL *et al.* (2011). IL-15 and type I interferon are required for activation of tumoricidal NK cells by virus-infected dendritic cells. *Cancer Res* **71**: 2497–2506.
- Melcher, A, Parato, K, Rooney, CM and Bell, JC (2011). Thunder and lightning: immunotherapy and oncolytic viruses collide. *Mol Ther* **19**: 1008–1016.
- Martin-Fontecha, A, Thomsen, LL, Brett, S, Gerard, C, Lipp, M, Lanzavecchia, A *et al.* (2004). Induced recruitment of NK cells to lymph nodes provides IFN-gamma for T(H)1 priming. *Nat Immunol* **5**: 1260–1265.
- Cooper, MA, Fehniger, TA and Caligiuri, MA (2001). The biology of human natural killer-cell subsets. *Trends Immunol* **22**: 633–640.
- Silva, A, Andrews, DM, Brooks, AG, Smyth, MJ and Hayakawa, Y (2008). Application of CD27 as a marker for distinguishing human NK cell subsets. *Int Immunol* **20**: 625–630.
- Wise, LM, Savory, LJ, Dryden, NH, Whelan, EM, Fleming, SB and Mercer, AA (2007). Major amino acid sequence variants of viral vascular endothelial growth factor are functionally equivalent during Orf virus infection of sheep skin. *Virus Res* **128**: 115–125.
- Balassa, TC and Robinson, AJ (1987). Orf virus replication in bovine testis cells: kinetics of viral DNA, polypeptide, and infectious virus production and analysis of virion polypeptides. *Arch Virol* **97**: 267–281.
- Wang, C, Barrett, JW, Stanford, M, Werden, SJ, Johnston, JB, Gao, X *et al.* (2006). Infection of human cancer cells with myxoma virus requires Akt activation via interaction with a viral ankyrin-repeat host range factor. *Proc Natl Acad Sci USA* **103**: 4640–4645.
- Stojdl, DF, Lichty, BD, tenOever, BR, Paterson, JM, Power, AT, Knowles, S *et al.* (2003). VSV strains with defects in their ability to shut down innate immunity are potent systemic anti-cancer agents. *Cancer Cell* **4**: 263–275.
- Willmon, C, Harrington, K, Kottke, T, Prestwich, R, Melcher, A and Vile, R (2009). Cell carriers for oncolytic viruses: Fed Ex for cancer therapy. *Mol Ther* **17**: 1667–1676.
- Kirstein, JM, Graham, KC, Mackenzie, LT, Johnston, DE, Martin, LJ, Tuck, AB *et al.* (2009). Effect of anti-fibrinolytic therapy on experimental melanoma metastasis. *Clin Exp Metastasis* **26**: 121–131.
- Chakrabarti, S, Brechling, K and Moss, B (1985). Vaccinia virus expression vector: coexpression of beta-galactosidase provides visual screening of recombinant virus plaques. *Mol Cell Biol* **5**: 3403–3409.
- Ohashi, PS, Oehen, S, Buerki, K, Pircher, H, Ohashi, CT, Odermatt, B *et al.* (1991). Ablation of “tolerance” and induction of diabetes by virus infection in viral antigen transgenic mice. *Cell* **65**: 305–317.